

# Determining orbital moments in antiferromagnets and paramagnets: a spin-resolved circularly-polarized photoemission study on CoO

G. Ghiringhelli<sup>1,2</sup>, L. H. Tjeng<sup>3</sup>, A. Tanaka<sup>4</sup>, O. Tjernberg<sup>1,5</sup>, T. Mizokawa<sup>3,6</sup>, J. L. de Boer<sup>7</sup>, and N. B. Brookes<sup>1</sup>

<sup>1</sup> *ESRF - European Synchrotron Radiation Facility, BP 220, 38043 Grenoble, France.*

<sup>2</sup> *INFM, Dipartimento di Fisica, Politecnico di Milano, piazza Leonardo da Vinci 32, 20133 Milano, Italy.*

<sup>3</sup> *Solid State Physics Laboratory, MSC, University of Groningen, Nijenborgh 4, 9747 AG Groningen, the Netherlands.*

<sup>4</sup> *Department of Quantum Matter, ADSM, Hiroshima University, 1-3-1 Kagamiyama, Higashi-Hiroshima 739-8526, Japan.*

<sup>5</sup> *Department of Physics, KTH, S-10044 Stockholm, Sweden.*

<sup>6</sup> *Department of Complexity Science and Engineering, University of Tokyo, Tokyo 113-0033, Japan.*

<sup>7</sup> *Chemical Physics Laboratory, MSC, University of Groningen, Nijenborgh 4, 9747 AG Groningen, the Netherlands.*

(October 13, 2000)

We have measured accurately the spin polarization in the integrated valence band photoemission spectrum of CoO using circularly polarized soft x-rays. This quantity is directly related to the expectation value of the 3d spin-orbit operator of the system in the initial state, from which the ratio between the orbital and spin contribution to the total magnetic moment can be deduced. While the measurement is sensitive to the magnetization axis, it does not require a net macroscopic magnetization nor the presence of a long range magnetic order, and is therefore suitable to extract orbital moments in transition metal antiferromagnets, as well as paramagnets and disordered systems.

Transition metal materials exhibit a wide range of fascinating magnetic and electronic properties, many of those governed by the intricate balance between band formation and atomic-like electron correlation effects, together with the interplay between charge, spin and orbital degrees of freedom. Spin-orbit interaction plays often an important role, for example, in determining the orientation of the magnetic moments relative to the crystal axes. Single-ion anisotropy phenomena are in particular interesting for the study of surface magnetism as well as for the research field of thin films and nano-structured materials, where the reduced dimensionality and the near presence of a different material may alter significantly the magnetic properties [1–3]. Spin-orbit interaction in combination with orbital ordering can also lead to novel and peculiar phenomena, such as the multiple temperature-induced magnetization reversals in YVO<sub>3</sub> [4]. The role of spin-orbit interaction should also not be neglected in the ruthenates [5], of which Sr<sub>2</sub>RuO<sub>4</sub> is a fascinating superconductor [6–8].

The measurement of the separate spin and orbital contributions to the magnetic moments in these materials is, however, far from trivial, especially for thin films, surfaces and nano-structured materials. It is not more than a decade ago that sum rules have been developed for magnetic soft x-ray dichroism, by which those separate contributions can be reliably determined for ferromagnetic materials [9–11]. And it is only very recently that the orbital moment in an ordered antiferromagnet like NiO have been successfully measured using magnetic x-ray scattering [12,13], due to the availability of very intense synchrotron radiation sources. In our present work, we set out to explore the feasibility of another spectroscopic technique, namely spin-resolved photoemission using cir-

cularly polarized soft x-rays. As we will show below, this technique is complementary in the sense that while it is sensitive to the magnetization axis, it does not need a net macroscopic magnetization or long range magnetic order, so that it is suitable not only for ferro- and antiferromagnets, but also for paramagnetic and crystallographically disordered systems, including in particular clusters and nano-structured materials, which often have the tendency to become superparamagnetic [14–16].

The principle of our photoemission technique is based on the Fano effect, i.e. the creation of spin-polarized electrons when circularly polarized light is used for the excitation, as a consequence of spin-orbit interaction and the dipole selection rules [17,18]. Instrumental for a quantitative analysis is the sum-rule derived by van der Laan and Thole [19], which relates the spin polarization of the integrated valence band photoemission spectrum to the expectation value of a spin-orbit operator of the system in the initial state:

$$\frac{\rho^{11}}{\rho^{00}} = \frac{2A_1 \langle \sum_i l_z(i) s_{z'}(i) \rangle}{A_0 \langle n \rangle} \quad (1)$$

where  $\rho^{00}$  is the integrated isotropic photoemission intensity and  $\rho^{11}$  is the so-called integrated spin-orbit intensity, defined as the difference between the integrated intensities taken with parallel and antiparallel alignment of the photon angular momentum and electron spin.  $\langle n \rangle$  is the number of electrons in the subshell under consideration, the index  $i$  runs over the electrons in the subshell, and the constants  $A_0$  and  $A_1$  depend on the transitions considered (e.g.  $A_0 = \frac{1}{5}$  and  $A_1 = -\frac{1}{15}$  for  $d \rightarrow f$  and  $A_0 = \frac{1}{5}$  and  $A_1 = \frac{1}{10}$  for  $d \rightarrow p$  [19]).  $\mathbf{z}$  gives the direction both of the Poynting vector of the light and of the quantization axis of the angular components, and  $\mathbf{z}'$  indicates the spin

quantization axis. The quantity  $\rho^{11}$  depends on the relative orientation of  $\mathbf{z}$ ,  $\mathbf{z}'$  and of the magnetization axis of the material, but a net macroscopic magnetization or long range magnetic order is not necessary for  $\rho^{11}$  to be non-zero. To be more precise for an isotropic system and  $\mathbf{z}=\mathbf{z}'$  it becomes  $\langle \sum_i l_z(i) s_z(i) \rangle = \frac{1}{3} \langle \sum_i \mathbf{l}_i \cdot \mathbf{s}_i \rangle$  [19].

If the photoemission spectra are not angle-integrated, but taken at a particular angle  $\theta$  with respect to  $\mathbf{z}$ , an angular dependent prefactor needs to be also included for the isotropic case:

$$\frac{\rho^{11}}{\rho^{00}} = \frac{3 - 4\cos^2\theta}{2 - \cos^2\theta} \cdot \frac{2A_1 \langle \sum_i \mathbf{l}(i) \cdot \mathbf{s}(i) \rangle}{3A_0 \langle n \rangle} \quad (2)$$

We note that at the magic angle, i.e.  $\theta \approx 54.7^\circ$ , the prefactor becomes identical to 1. For practical purposes the real measurements are usually made using only circularly polarized x-rays, thus disregarding the contribution of the linearly polarized light. In such a case the measured quantity  $\Pi$  is the ratio between the difference and the sum of the integrated spectra taken with parallel and antiparallel alignment of the photon angular momentum and photoelectron spin. The expressions of equations (1) and (2) can then be used by considering  $\frac{\rho^{11}}{\rho^{00}} \approx \frac{2}{3}\Pi$ .

To test the feasibility of this photoemission technique, we chose CoO, which could serve as a model system for transition metal materials. It has a very intriguing magnetic structure and tetragonal lattice deformations of the rocksalt crystal structure below the antiferromagnetic ordering temperature [20–25], for which it is thought that the spin-orbit interaction plays a crucial role [26–28]. Until now, only the total magnetic moment is known experimentally ( $3.4 - 3.8\mu_B$ ) [22–24,29], whereas the separate spin and orbital contributions have been estimated only theoretically by using band structure calculations [30,31]. As a start, we have carried out the measurements at 390 K, far above the Néel temperature ( $T_N \approx 290$  K), in order to avoid magnetic domain structure issues, which otherwise could have complicated the analysis. In addition, this way of measuring allows us to show that the technique is suitable to determine orbital moments in systems without long range order, e.g. in the paramagnetic state.

The experiments were performed using the helical undulator [32] based beamline ID12B [33] at the European Synchrotron Radiation Facility (ESRF) at Grenoble. The spectra were recorded using a 140 mm mean radius hemispherical analyzer coupled to a mini-Mott 25 kV spin polarimeter [34]. The photon energy was set to 600 eV, and the degree of circular polarization was  $\approx 85\%$ . The combined energy resolution for the measurements was 0.6 eV, and the spin detector had an efficiency (effective Sherman function) of 17%. The high sensitivity of this new detector was essential for the success of these measurements. The angle  $\theta$  between the photon beam and the analyzer was  $60^\circ$ , and the angle formed by  $\mathbf{z}$  and

$\mathbf{z}'$  was  $30^\circ$ . The sample was a single crystal CoO cleaved *in situ*, and the measurement was carried out at normal emission from the (001) surface. The spin-resolved spectra were recorded for the two spin directions (measured simultaneously) and for both light polarizations in order to eliminate systematic errors. The pressure of the spectrometer chamber was  $1 \times 10^{-10}$  mbar.

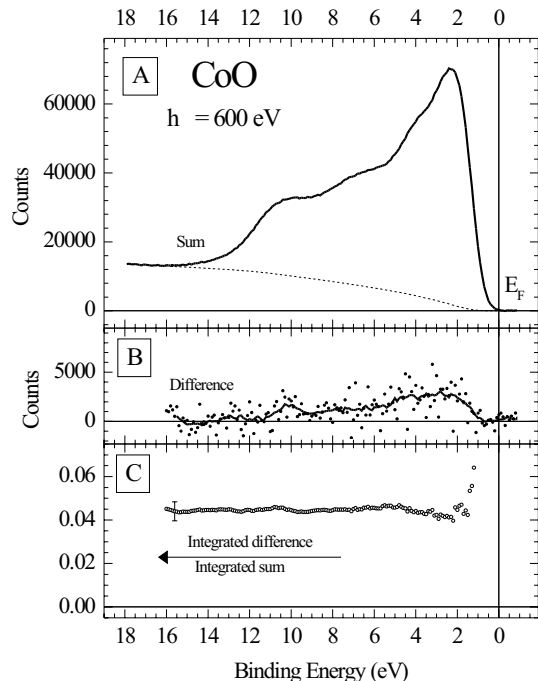


FIG. 1. Spin polarized photoemission spectrum of CoO measured with circularly polarized light ( $h\nu = 600$  eV). The solid line in Panel A shows the sum of two spectra, one taken with parallel and the other with anti-parallel alignment of photon angular momentum and electron spin. The dots in Panel B depict the difference between the two spectra, with the solid line (5 point average) as a guide to the eye. The small circles in Panel C give the ratio between the integrated difference and the integrated sum spectrum, where the integration is carried out from the Fermi level ( $E_F$ ) to higher binding energies, after removing a background from the sum spectrum (dashed line in panel A). The statistical error in the ratio at convergence is also shown.

The top panel of figure 1 shows the unpolarized valence band photoemission spectrum of CoO, which is the sum of spectra taken with parallel and antiparallel alignment of the photon angular momentum and electron spin. It is almost identical to the spectra taken with unpolarized x-rays and photon energy of 1253.6 eV and 1486.6 eV in earlier studies [35,36]. The middle panel depicts the difference between the spectra taken with parallel and antiparallel alignment of the photon angular momentum and electron spin, after taking into account the spin detector efficiency and the degree of circular polarization. The quantity of interest  $\Pi$  is the ratio between the integrated difference spectrum and the integrated sum spec-

trum. Carrying out the integration from 0 eV to higher binding energies,  $\Pi$  converges to  $0.045 \pm 0.005$  as shown in the bottom panel. Here the usual integral background correction has been made for the sum spectrum as depicted by the dashed line in the top panel. The error bar is estimated from the statistics given by the total number of counts before any background subtraction.

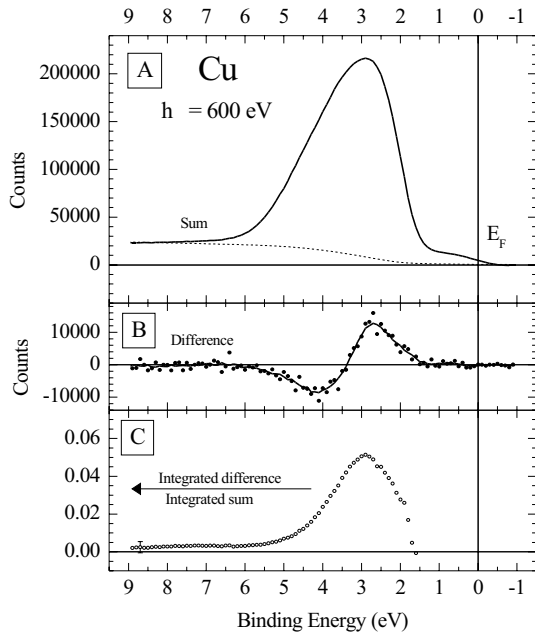


FIG. 2. Spin polarized photoemission spectrum of Cu measured with circularly polarized light ( $h\nu = 600$  eV). See caption of figure 1 for details.

To verify the reliability of the measurement, we have also carried out the experiment on polycrystalline Cu metal, for which we expect a null result ( $\Pi = 0$ ). In fact, although the  $3d$  spin-orbit interaction is even stronger in Cu than in Co, the spin-orbit operator expectation value, when evaluated over the closed  $3d$  subshell, must be zero as the orbital and spin moments. Nevertheless the polarization spectrum can show non-zero features due to the energy splitting of the  $3d$  states holding opposite spin-orbit coupling. The results are shown in figure 2. The presence of the spin-orbit interaction in the Cu  $3d$  shell can be clearly seen in the difference spectrum. In this case we find that  $\Pi$  converges to  $0.002 \pm 0.003$ . This ratio is essentially zero within the very small statistical error, proving that the experiment has been set up correctly and that the above mentioned results for CoO are reliable.

In analyzing the CoO results in terms of Co  $3d$  magnetic moments, we note that the contribution of the O  $2p$  to the integrated intensity of the difference spectrum is completely negligible, since the O  $2p$  shell is essentially closed. Moreover, it has a much smaller spin-orbit coupling strength than the Co  $3d$ . The contribution to the integrated intensity of the sum spectrum is small but not

negligible: using MgO as a reference sample, we measured that at 600 eV photons the O  $2p$  contributes about 15% to the integrated eV CoO valence band spectrum. Subtracting this out, we arrive at  $\Pi = 0.053 \pm 0.006$  and  $\frac{\rho^{11}}{\rho^{00}} = 0.035 \pm 0.04$ .

For a photoemission process from a  $3d$  shell, like in CoO, we have to consider transitions to both  $\epsilon f$  and  $\epsilon p$  like final states. The quotient  $A_1/A_0$  in equation (2), which is  $-\frac{1}{3}$  for  $d \rightarrow f$  and  $\frac{1}{2}$  for  $d \rightarrow p$ , has to be replaced by  $(-1 + R_{pf})/(3 + 2R_{pf})$ , where  $R_{pf}$  is the photon energy dependent cross-section of the  $3d \rightarrow \epsilon p$  transition relative to that of the  $3d \rightarrow \epsilon f$ . At 600 eV  $R_{pf}$  is about 0.04 [37], meaning that the transitions are predominantly of  $3d \rightarrow \epsilon f$  character. Together with  $\theta = 60^\circ$  and a  $d$ -occupation number  $\langle n \rangle \approx 7.1$  for CoO [37], we then find from equation 2 that the observed Co spin polarization corresponds to  $\langle \sum_i \mathbf{l}_i \cdot \mathbf{s}_i \rangle \approx -1.05 \pm 0.12$  (in units of  $\hbar^2$ ). This is a very large number, indicating the importance of the spin-orbit interaction, and thus also confirming the basic assumption of the various models [26–28] explaining the unique magnetic and lattice structure of CoO.

In order to extract further numbers as far as local properties are concerned, we have performed model calculations using a CoO<sub>6</sub> cluster in  $O_h$  symmetry [37]. Here the hybridization between the Co  $3d$  and the O  $2p$  orbitals is included, as well as the hybridization among the O  $2p$  orbitals at neighboring O sites and the effect of the temperature on the population of the lowest energy states. We have incorporated the full atomic multiplet theory for the Co  $3d$ , in order to account for the orbital and spin dependent on-site Coulomb and exchange interactions. As a starting point, we have used parameter values previously determined from various spectroscopic measurements [37,38]. By fine tuning the 10  $Dq$  crystal field value to 0.5 eV we were able to reproduce accurately the experimental value at  $T = 390$  K:  $\Pi = 0.053$ . Although in the real sample  $\langle L_z \rangle = 0$  and  $\langle S_z \rangle = 0$  for  $T > T_N$ , we can simulate a magnetic ordering even above  $T_N$  by switching on a molecular field: the cluster model calculation gives, using the optimized parameters,  $\frac{\langle L_z \rangle}{\langle S_z \rangle} \approx 0.77$  at  $T = 390$  K. This result demonstrates again the importance of spin-orbit interaction in CoO. The calculations at  $T = 0$  K, using a molecular field of 37 meV, give  $\frac{\langle L_z \rangle}{\langle S_z \rangle} \approx 1.04$ . By combining this value with the known total magnetic moment of  $3.81 \mu_B$  we can easily derive  $\langle L_z \rangle = 1.31 \hbar$  and  $\langle S_z \rangle = 1.25 \hbar$ .

While cluster calculations provide an accurate method to extract local magnetic quantities from the measurements of  $\langle \sum_i l_z(i) s_z'(i) \rangle$  or  $\langle \sum_i \mathbf{l}_i \cdot \mathbf{s}_i \rangle$ , we also propose two methods for relating the measured  $\Pi$  to some approximated values of the orbital and spin angular moments. Although less accurate, these approximations may give a more direct insight about the experimental results and, by avoiding the need for model calculations, may facilitate a wider application of this technique for materials

science. We will consider here two distinct cases: the first is for a material in the paramagnetic state and the second is for a single domain material with long range magnetic order, be it ferro-, antiferro- or ferrimagnetic in nature. We will use the cluster calculations to test these approximations.

For the paramagnetic state, the relevant quantity to be analyzed is  $\langle \sum_i \mathbf{l}_i \cdot \mathbf{s}_i \rangle$ . From the CoO cluster calculations, we find that  $\langle \mathbf{S}^2 \rangle = 3.51\hbar^2$  and  $\langle \mathbf{L}^2 \rangle = 11.57\hbar^2$  at  $T = 390$  K. These values are very close to the free ion values of  $\langle \mathbf{S}^2 \rangle = 3.75\hbar^2$  and  $\langle \mathbf{L}^2 \rangle = 12.00\hbar^2$ . This shows that the main component of the  ${}^4T_1$  like (near) ground state of the  $\text{Co}^{2+}$  ion in CoO [36] is still given by the  ${}^4F$  state. For such a lowest multiplet state in spherical symmetry it can be shown that  $\langle \mathbf{L} \cdot \mathbf{S} \rangle = \pm 2S \langle \sum_i \mathbf{l}_i \cdot \mathbf{s}_i \rangle$ , where the plus (minus) sign is for a less (more) than half filled shell [39]. Making in addition the crude approximation that the magnetic moment  $\mathbf{M} = \mathbf{L} + 2\mathbf{S}$  is determined mostly by the spin contribution, we can write  $\frac{\langle L_z \rangle}{\langle S_z \rangle} = \frac{\langle \mathbf{L} \cdot \mathbf{M} \rangle}{\langle \mathbf{S} \cdot \mathbf{M} \rangle} \approx \frac{\langle \mathbf{L} \cdot \mathbf{S} \rangle}{\langle \mathbf{S} \cdot \mathbf{S} \rangle} = \pm 2S \frac{\langle \sum_i \mathbf{l}_i \cdot \mathbf{s}_i \rangle}{\langle \mathbf{S}^2 \rangle}$ . For the CoO case with  $S = \frac{3}{2}$ , this gives  $\frac{\langle L_z \rangle}{\langle S_z \rangle} \approx (-3) \times (-\frac{1.05}{3.75}) = 0.84$  at  $T = 390$  K, which is not so far from the ratio directly calculated from the cluster model above, namely 0.77. We expect that this crude approximation to work rather well for magnetic insulators with suppressed charge fluctuations and small orbital moments. Using for instance the  $\text{NiO}_6$  cluster model for NiO, the approximation provides  $\frac{\langle L_z \rangle}{\langle S_z \rangle} \approx 0.33$  to be compared with 0.35 as directly obtained and to 0.34 as measured in ref. [12].

For the magnetically ordered state, we consider the case where  $\mathbf{z} = \mathbf{z}'$  and the sample has its magnetization direction along  $\mathbf{z}$ . The quantity to be analyzed is then  $\langle \sum_i l_z(i) s_z(i) \rangle$ . Assuming that the valence majority spin states are completely filled [40], we can write  $\langle \sum_i l_z(i) s_z(i) \rangle = -\frac{1}{2}\hbar \langle \sum_i l_z(i) \rangle = -\frac{1}{2}\hbar \langle L_z \rangle$ . We find from the  $\text{CoO}_6$  cluster calculations above that  $\langle \sum_i l_z(i) s_z(i) \rangle = -0.67\hbar^2$  at  $T = 0$  K. The approximation therefore gives  $\langle L_z \rangle \approx -0.67\hbar^2 / (-\frac{1}{2}\hbar) = 1.33\hbar$ , which is in very good agreement with the  $\langle L_z \rangle$  value calculated directly for the ground state of the cluster, namely  $1.31\hbar$ . This analysis shows therefore that an accurate evaluation of  $\langle L_z \rangle$  can be made even without knowing the total magnetic moment provided that the measurement can be made on a single magnetic domain.

To conclude, we have shown how the integrated spin polarization of the valence band photoemission spectrum can be actually related to the expectation value of a spin-orbit operator in the initial state. For systems with suppressed charge fluctuations, such as magnetic insulators, we have shown that the ratio between the orbital and spin contribution to the total magnetic moment can be accurately deduced using cluster calculations. In addition, we have shown that under simple assumptions it is possible to derive an approximate value for the orbital moment directly from the experimental data, even

without the support of model calculations, both for the magnetically disordered and ordered state. Whether or not the the present analysis can be extended to metallic transition metal materials is not clear at the moment, and further study is highly desired, both experimentally and theoretically.

We would like to thank K. Larsson for his invaluable technical assistance.

- 
- [1] J. Shen *et al.*, Phys. Rev. B **56**, 2340 (1997); *ibid.* 11134.
  - [2] J. Dorantes-Dávila and G.M. Pastor, Phys. Rev. Lett. **81**, 208 (1998).
  - [3] P. Ohresser *et al.*, Phys. Rev. B **62**, 5803 (2000).
  - [4] Y. Ren *et al.*, Nature **396**, 441 (1998).
  - [5] T. Mizokawa *et al.*, submitted to Phys. Rev. Lett.
  - [6] Y. Maeno *et al.*, Nature **372**, 532 (1994).
  - [7] A. P. Mackenzie *et al.*, Phys. Rev. Lett. **80**, 161 (1998).
  - [8] T. M. Rice and M. Sigrist, J. Phys.: Condens. Matter **7**, L643 (1995).
  - [9] B. T. Thole *et al.*, Phys. Rev. Lett. **68**, 1943 (1992).
  - [10] P. Carra *et al.*, Phys. Rev. Lett. **70**, 694 (1993).
  - [11] C. T. Chen *et al.*, Phys. Rev. Lett. **75**, 152 (1995).
  - [12] V. Fernandez *et al.*, Phys. Rev. B **57**, 7870 (1998).
  - [13] D. Gibbs *et al.*, Phys. Stat. Sol. (b) **215**, 667 (1999).
  - [14] F. C. Voogt *et al.*, Phys. Rev. B **57**, R8107 (1998).
  - [15] S. Padovani *et al.*, Phys. Rev. B **59**, 11887 (1999).
  - [16] O. Fruchart *et al.*, Phys. Rev. Lett. **83**, 2769 (1999).
  - [17] U. Fano, Phys. Rev. **178**, 131 (1969); **184**, 250 (1969).
  - [18] C. M. Schneider and J. Kirschner, Critical Reviews in Solid State and Materials Sciences **20**, 179 (1995).
  - [19] G. van der Laan and B. T. Thole, Phys. Rev. B **48**, 210 (1993).
  - [20] C. G. Shull *et al.*, Phys. Rev. **83**, 333 (1951).
  - [21] Y-Y. Li, Phys. Rev. **100**, 627 (1955).
  - [22] W. L. Roth, Phys. Rev. **110**, 1333 (1958); **111**, 772 (1958).
  - [23] B. van Laar, Phys. Rev. **138**, A584 (1965).
  - [24] D. C. Khan and R. A. Erickson, Phys. Rev. B **1**, 2243 (1970).
  - [25] M. D. Rechten *et al.*, Phys. Rev. Lett. **24**, 1485 (1970).
  - [26] J. Kanamori, Prog. Theor. Phys. **17**, 177 (1957).
  - [27] T. Nagayima and K. Motizuki, Rev. Mod. Phys. **30**, 89 (1958).
  - [28] T. Shishidou and T. Jo, J. Phys. Soc. Jpn. **67**, 2637 (1998).
  - [29] D. Herrmann-Ronzaud *et al.*, J. Phys. C: Solid State Phys., **11**, 2123 (1978).
  - [30] A. Svane and O. Gunnarsson, Phys. Rev. Lett. **65**, 1148 (1990).
  - [31] I. V. Solovyev *et al.*, Phys. Rev. Lett. **80**, 5758 (1998).
  - [32] P. Elleaume, J. Synchrotron Radiat. **1**, 19 (1994).
  - [33] J. Goulon *et al.*, Physica (Amsterdam) **208B**, 199 (1995).
  - [34] G. Ghiringhelli *et al.*, Rev. Sci. Instrum. **70**, 4225 (1999).
  - [35] Z.-X. Shen *et al.*, Phys. Rev. B **42**, 1817 (1990).
  - [36] J. van Elp *et al.*, Phys. Rev. B **44**, 6090 (1991).

- [37] A. Tanaka and T. Jo, J. Phys. Soc. Jpn. **63**, 2788 (1994).
- [38] The parameter values used in the model calculations are  $\Delta=6.5\text{eV}$ ,  $U_{3d3d}=6.5\text{eV}$ ,  $V(E_g)=2.0\text{eV}$ ,  $10Dq=0.5\text{eV}$ , with the Slater integrals given by 80% of their Hartree-Fock values and the Co  $\xi_{3d}$  by the full Hartree-Fock value. All  $\Delta$  and  $U$  values are given with respect to the multiplet average.
- [39] *Multiplets of Transition-Metal Ions in Crystals*, by S. Sugano, Y. Tanabe, and H. Kamimura, (Academic Press, New York, 1970).
- [40] T. Jo and S. Imada, J. Phys. Soc. Jpn. **67**, 3617 (1998).